2024 IEEE 63rd Conference on Decision and Control (CDC)
December 16-19, 2024. MiCo, Milan, Italy

Distributed Robust Indirect Adaptive Control for Manipulation of a Passive Object by a Group of Robotic Agents

Jacopo Giordano, Angelo Cenedese and Andrea Serrani

***Abstract*— In this work, a distributed indirect adaptive controller is designed for a group of robotic agents cooperatively manipulating a common payload. Uncertainty on the model of the manipulated object and limited actuation capabilities of the single agents can significantly impact the overall behavior of the control system. An indirect adaptive control scheme is proposed in this paper to address these shortcomings. In particular, model uncertainty and loss of effectiveness of the actuators are handled in a unifying fashion by an adaptive control architecture that preserves physical consistency of the estimated inertial parameters of the manipulated object, while simultaneously providing an anti-windup mechanism for the estimated inertial parameters against actuator saturation. The stability of the closed loop system is proven theoretically and the performance and robustness of the control system are validated by means of comparative simulations with respect to a baseline state-of-the-art controller.**

I. Introduction

In certain application domains, manipulating an object via coordination of multiple agents may be more advantageous or even necessary than manipulation via a single agent [1]. It is therefore unsurprising that cooperative manipulation has attracted considerable attention in the robotics community. Early work involves multi-arm robots with only a few agents and centralized architectures, and relies on complete knowledge of the system dynamics. Recent efforts attempt at relaxing such requirement. Specifically, in [2], a fully decentralized robust control solution is designed for cooperatively manipulating a shared load on a plane. Therein, a decentralized estimator is employed to identify the inertial parameters of the manipulated object. Similarly, the authors of [3] propose a preliminary identification stage during which the object is moved via specific contact wrenches to estimate the kinematic and dynamic parameters of the object. A distributed force controller is then developed to regulate the tracking error and limit the internal forces on the object. In [4], a passivity-based control design is proposed to deal with the unknown manipulated object and environment.

Adaptive control has emerged as an alternative approach to off-line systems identification when dealing with model uncertainty arising from an unknown manipulated object. Among early works employing adaptive technique, [5] and [6] employ adaptation within a centralized robust control architecture. More recently, the authors of [7] proposed an adaptive decentralized direct controller handling parameter uncertainties of both the agents and the manipulated object. It is noted, however, that uncertainty on the point of grasp of each individual agent was not considered, as only masses and inertia parameters were subjected to adaptation. In [8], the previously cited method is extended to the case where also the position of the center of mass of the payload and the grasping points are assumed to be unknown. However, in contrast to the previous work, the dynamics of the manipulators were not considered.

Two distinct approaches to adaptive control exist: direct and indirect adaptive control. In the former approach, the parameters of the controller are adjusted online based on the output of an error system. In the latter technique, the model parameters are adjusted online using a predictor of the plant model, and the controller gains are updated accordingly. To the best of the authors knowledge, none of the works present in the literature consider an indirect adaptive approach to simultaneously dealing with model uncertainties (including the manipulated object) and the presence of non-negligible adversarial actuators effects. The lack of popularity of indirect adaptive control schemes in robotics applications can be traced to the necessity of guaranteeing at all times invertibility of the estimated inertia matrix for a predictor of the robotics dynamics to be employed. To fill this gap, this work presents a novel distributed indirect adaptive control scheme for a group of N cooperating agents manipulating a common payload. Input saturation and agent efficiency are directly considered alongside uncertainty on the location of the points of grasp in a control architecture comprising an observer-based dynamic estimator. Moreover, inspired from [9], a *natural adaptation law* is employed for updating online the inertial parameters of the manipulated object while preserving their physical consistency. This results in an estimated inertia matrix which is invertible at each time instant, thus allowing a simple implementation of the predictor.

II. Assumptions and Notation

A. System and Environmental Assumptions

Similarly to the works [7], [8] the manipulated object is considered to be passive and rigid, that is, it is not equipped with any actuator and does not deform when wrenches are applied. The object is manipulated from N contact points, one for each autonomous agent acting on it. The grasps are considered to be firm, allowing a full wrench to be applied at each contact point. It is assumed that all the cooperating agents are able to measure or receive from a leader agent

Jacopo Giordano and Angelo Cenedese are with the Department of Information Engineering, University of Padua, Italy. Email: jacopo.giordano@phd.unipd.it, cenedese@dei.unipd.it
Andrea Serrani is with the Department of Electrical & Computer Engineering, The Ohio State University, Columbus, OH 43210. Email: serrani.1@osu.edu
Corresponding Author: Jacopo Giordano.

979-8-3503-1632-2/24/$31.00 ©2024 IEEE

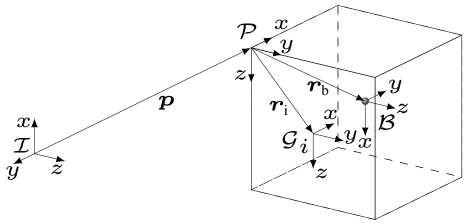

Fig. 1: Passive object with the indication of the frames of interest.

the pose and velocity of a point on the manipulated object called the *measurement point with respect to the inertial frame*. The trajectory followed by the manipulated object is assumed to be available to each agent. The uncertain inertial parameters of the grasped object are assumed to range within a known compact set. The effect of gravity is not considered in this work. If necessary, it could easily be incorporated as an external force applied to the system, to be compensated by the manipulating agents.

B. Notation

The main reference frames and vectors used throughout this work are shown in Fig. 1, where frame $\mathcal{I}$ represents the inertial frame. First, a body-fixed frame $\mathcal{P}$ is placed at the measurement point. A second body-fixed frame $\mathcal{B}$ is placed at the center of mass of the passive object, and is aligned with frame $\mathcal{P}$. The position of the i^{th} grasping point, with $i = 1, \ldots, N$, is identified by the origin of frame $\mathcal{G}_i$. Without loss of generality, in order to simplify the notation, the $\mathcal{G}_i$ frames are also aligned with frame $\mathcal{P}$. The vector $\boldsymbol{p} \in \mathbb{R}^3$ represents the position of the measurement point with respect to the origin of the inertial frame $\mathcal{I}$, expressed in inertial coordinates. The orientation of frame $\mathcal{P}$ with respect to the inertial frame $\mathcal{I}$ is described by the rotation matrix $\boldsymbol{R} \in SO(3)$. The linear and angular velocities of the measurement point with respect to the inertial frame $\mathcal{I}$, expressed in inertial coordinates, are denoted by $\boldsymbol{v} \in \mathbb{R}^3$ and $\boldsymbol{\omega} \in \mathbb{R}^3$, respectively. The wrench applied at the measurement point, expressed in $\mathcal{I}$-coordinates, is represented by $\boldsymbol{\tau}_p = \left[\boldsymbol{f}_p^T, \boldsymbol{t}_p^T\right]^T \in \mathbb{R}^6$, where $\boldsymbol{f}_p \in \mathbb{R}^3$ and $\boldsymbol{t}_p \in \mathbb{R}^3$ are the force and torque components, respectively. The position of the i^{th} grasping point and center of mass of the passive object with respect to the measurement point (expressed in $\mathcal{P}$ coordinates) are represented by the vectors $\boldsymbol{r}_i \in \mathbb{R}^3$ and $\boldsymbol{r}_b \in \mathbb{R}^3$, respectively. The mass and inertia matrix of the manipulated object with respect to frame $\mathcal{P}$ are denoted by the symbols $m \in \mathbb{R}$ and $\boldsymbol{I} \in \mathbb{R}^{3\times3}$, respectively. The $n \times n$ identity matrix and zero matrix are respectively denoted by with $\mathbb{I}_{n\times n}$ and $\mathbb{O}_{n\times n}$. The Euclidean norm is denoted by $|\boldsymbol{x}| = \sqrt{\boldsymbol{x}^T\boldsymbol{x}}$, $\boldsymbol{x} \in \mathbb{R}^n$. Finally, the infinity and asymptotic norms of a signal $\boldsymbol{x}(\cdot)$ are defined as follows:

$$||\boldsymbol{x}(\cdot)||_\infty := \sup_{t\geq0} |\boldsymbol{x}(t)|, \qquad ||\boldsymbol{x}(\cdot)||_a := \limsup_{t\to0} |\boldsymbol{x}(t)|$$

III. System Dynamics

The dynamical model describing the motion of the passive object referred to the measurement point can be readily derived using the Newton-Euler formulation [8]

$$\boldsymbol{M}(\boldsymbol{x})\ddot{\boldsymbol{x}} + \boldsymbol{C}(\boldsymbol{x}, \dot{\boldsymbol{x}})\dot{\boldsymbol{x}} = \boldsymbol{\tau}_p \tag{1}$$

with

$$\boldsymbol{M}(\boldsymbol{x}) = \begin{bmatrix} m\mathbb{I}_{3\times3} & -m\left[\boldsymbol{R}\boldsymbol{r}_b\right]_\times \\ m\left[\boldsymbol{R}\boldsymbol{r}_b\right]_\times & \boldsymbol{R}\boldsymbol{I}\boldsymbol{R}^T \end{bmatrix}$$

$$\boldsymbol{C}(\boldsymbol{x}, \dot{\boldsymbol{x}}) = \begin{bmatrix} \mathbb{O}_{3\times3} & -m\left[\boldsymbol{\omega}\right]_\times\left[\boldsymbol{R}\boldsymbol{r}_b\right]_\times \\ \left[\boldsymbol{\omega}\right]_\times\left[\boldsymbol{R}\boldsymbol{r}_b\right]_\times & \left[\boldsymbol{\omega}\right]_\times \boldsymbol{R}\boldsymbol{I}\boldsymbol{R}^T - m\left[\left[\boldsymbol{R}\boldsymbol{r}_b\right]_\times \boldsymbol{v}\right]_\times \end{bmatrix}$$

where $[\cdot]_\times$ is the skew symmetric matrix representing the cross product $[\boldsymbol{v}]_\times\boldsymbol{\omega} = \boldsymbol{v} \times \boldsymbol{\omega}$ with $\boldsymbol{v}, \boldsymbol{\omega} \in \mathbb{R}^3$, and $\boldsymbol{x} := (\boldsymbol{p}, \boldsymbol{R}) \in \mathbb{R}^3 \times SO(3)$ is the pose of the manipulated rigid body. With a mild abuse of notation, generalized velocities and accelerations are denoted by $\dot{\boldsymbol{x}} := \left[\boldsymbol{v}^T, \boldsymbol{\omega}^T\right]^T \in \mathbb{R}^6$ and $\ddot{\boldsymbol{x}} := \left[\dot{\boldsymbol{v}}^T, \dot{\boldsymbol{\omega}}^T\right]^T \in \mathbb{R}^6$, respectively. The matrix $\boldsymbol{M}(\boldsymbol{x}) \in \mathbb{R}^{6\times6}$ is the inertia matrix and $\boldsymbol{C}(\boldsymbol{x}, \dot{\boldsymbol{x}}) \in \mathbb{R}^{6\times6}$ is the matrix of Coriolis and centrifugal forces and torques.

A. Linear formulation with respect to the inertial parameters

It is well known that the right-hand side of equation (1) admits a linear parametrization with respect to the inertial parameters of the manipulated object of the form

$$\boldsymbol{Y}_\theta(\boldsymbol{x}, \dot{\boldsymbol{x}}, \ddot{\boldsymbol{x}})\boldsymbol{\theta} = \boldsymbol{M}(\boldsymbol{x}, \boldsymbol{\theta})\ddot{\boldsymbol{x}} + \boldsymbol{C}(\boldsymbol{x}, \dot{\boldsymbol{x}}, \boldsymbol{\theta})\dot{\boldsymbol{x}} \tag{2}$$

where $\boldsymbol{Y}_\theta(\boldsymbol{x}, \dot{\boldsymbol{x}}, \ddot{\boldsymbol{x}}) \in \mathbb{R}^{6\times10}$ is a regressor and $\boldsymbol{\theta} \in \Theta$ is a vector collecting all inertia parameters where $\Theta \subset \mathbb{R}^{10}$ is a known compact and convex set. Specifically, $\boldsymbol{\theta}$ is given by

$$\boldsymbol{\theta} = \left[m, \boldsymbol{h}_c^T, I^{xx}, I^{yy}, I^{zz}, I^{xy}, I^{yz}, I^{zx}\right]^T$$

where $\boldsymbol{h}_c := m\boldsymbol{r}_b \in \mathbb{R}^3$ and $I^{\alpha\beta} \in \mathbb{R}$ are the entries of the inertia matrix $\boldsymbol{I}$. The set of physically consistent inertial parameters [10] does not span the entirety of $\mathbb{R}^{10}$, but only a subset $\mathcal{M} \subset \mathbb{R}^{10}$ which is convex as well [9]. For later use, let $\mathcal{M}_c := \mathcal{M} \cap \Theta$ be the set of physically consistent parameters within the set Θ.

B. Actuators dynamics

The passive object is manipulated from the N grasping points. Consequently, the right-hand side of equation (1) is rewritten as follows [8]

$$\boldsymbol{\tau}_p = \sum_{i=1}^{N} \boldsymbol{\tau}_{p_i} = \sum_{i=1}^{N} \boldsymbol{H}(\boldsymbol{R}, \boldsymbol{r}_i)\boldsymbol{\tau}_{g_i} \tag{3}$$

where $\boldsymbol{\tau}_{p_i} \in \mathbb{R}^6$ is the portion of the wrench $\boldsymbol{\tau}_p$ applied by the i^{th} agent at the measurement point, and

$$\boldsymbol{H}(\boldsymbol{R}, \boldsymbol{r}_i) = \begin{bmatrix} \mathbb{I}_{3\times3} & \mathbb{O}_{3\times3} \\ \left[\boldsymbol{R}\boldsymbol{r}_i\right]_\times & \mathbb{I}_{3\times3} \end{bmatrix} \in \mathbb{R}^{6\times6}$$

is the grasp matrix mapping the wrench $\boldsymbol{\tau}_{g_i}$ applied at the grasping point $\boldsymbol{r}_i$ to the resulting wrench $\boldsymbol{\tau}_{p_i}$.

Property 1. *The following properties of the grasp matrix arise from its structure and the linearity of the $[\cdot]_\times$ operator:*

a) $\boldsymbol{H}(\boldsymbol{R}, \boldsymbol{r}_a)\boldsymbol{H}(\boldsymbol{R}, \boldsymbol{r}_b) = \boldsymbol{H}(\boldsymbol{R}, \boldsymbol{r}_a + \boldsymbol{r}_b)$
b) *The grasp matrix is always invertible, since it consists of a lower left triangular matrix with positive elements on its diagonal and it holds $\boldsymbol{H}^{-1}(\boldsymbol{R}, \boldsymbol{r}) = \boldsymbol{H}(\boldsymbol{R}, -\boldsymbol{r})$*

c) *There exist a regressor* $\boldsymbol{Y}_r(\boldsymbol{R},\boldsymbol{\tau}) \in \mathbb{R}^{6\times 3}$ *such that* $\boldsymbol{H}(\boldsymbol{R},\boldsymbol{r})\boldsymbol{\tau} = \boldsymbol{\tau} + \boldsymbol{Y}_r(\boldsymbol{R},\boldsymbol{\tau})\boldsymbol{r}$ *holds*

The dynamics of the agents generating the wrenches $\boldsymbol{\tau}_{g_i}$, $i = 1,\dots,N$ can be very different depending on the scenario considered. However, it is reasonable to assume that every agent is able to produce a wrench that is limited in magnitude, and the actuators are subject to possible loss of efficiency related to performance degradation. On the basis of these considerations, equation (3) is rewritten as

$$\boldsymbol{\tau}_p = \sum_{i=1}^{N} \boldsymbol{H}(\boldsymbol{R},\boldsymbol{r}_i)\boldsymbol{\Lambda}_i \mathrm{sat}_i(\boldsymbol{u}_i^{\mathrm{cmd}}) \tag{4}$$

where $\boldsymbol{u}_i^{\mathrm{cmd}}$ is the wrench applied at $\mathcal{G}_i$ by the i^{th} agent, $\mathrm{sat}_i(\cdot)$ is the saturation function of the i^{th} agent, and $\boldsymbol{\Lambda}_i = \mathrm{diag}(\boldsymbol{\lambda}_i) \in \mathbb{R}^{6\times 6}$ represents the efficiency of the actuation provided by the i^{th} agent. The vector $\boldsymbol{\lambda}_i$ collecting the entries on the diagonal of $\boldsymbol{\Lambda}_i$ ranges in the convex and compact set $\Lambda := \{\boldsymbol{\lambda}_i \in \mathbb{R}^6 | \lambda_{\min} \le \lambda_{i,j} \le 1 \text{ with } j = 1,\dots,6 \text{ and } \lambda_{\min} \in (0,1]\}$. In addition, the vectors $\boldsymbol{r}_i$ are assumed to range on a convex and compact set $R \subset \mathbb{R}^3$.

Using the property (1.a) and linearity, it is possible to rewrite equation (4) in two new forms, one that is more suitable for estimation (5a) and the other for control (5b)

$$\begin{aligned}\boldsymbol{\tau}_{p_i} &= \boldsymbol{H}(\boldsymbol{R},\boldsymbol{r}_i)\boldsymbol{\Lambda}_i\boldsymbol{u}_i = \boldsymbol{\Lambda}_i\boldsymbol{u}_i + \boldsymbol{Y}_r(\boldsymbol{R},\boldsymbol{\Lambda}_i\boldsymbol{u}_i)\boldsymbol{r}_i \\ &= \boldsymbol{Y}_\lambda(\boldsymbol{u}_i)\boldsymbol{\lambda}_i + \boldsymbol{Y}_\rho(\boldsymbol{R},\boldsymbol{u}_i)\boldsymbol{\rho}_i \qquad (5a) \\ &= \bar{\boldsymbol{H}}(\boldsymbol{R},\boldsymbol{\lambda}_i,\boldsymbol{\rho}_i)\boldsymbol{u}_i \qquad (5b)\end{aligned}$$

where $\boldsymbol{u}_i := \mathrm{sat}_i(\boldsymbol{u}_i^{\mathrm{cmd}})$ is the i^{th} saturated commanded control input, $\boldsymbol{Y}_\lambda(\boldsymbol{u}_i) \in \mathbb{R}^{6\times 6}$ and $\boldsymbol{Y}_\rho(\boldsymbol{R},\boldsymbol{u}_i) \in \mathbb{R}^{6\times 9}$ are two regressors, $\boldsymbol{\rho}_i = [\boldsymbol{r}_i^T\lambda_{i,1}, \boldsymbol{r}_i^T\lambda_{i,2}, \boldsymbol{r}_i^T\lambda_{i,3}]^T \in \mathcal{R}$ where $\mathcal{R} \subset \mathbb{R}^9$ is a known compact and convex set, and $\bar{\boldsymbol{H}}(\boldsymbol{R},\boldsymbol{\lambda}_i,\boldsymbol{\rho}_i) \in \mathbb{R}^{6\times 6}$. It is noted that $\bar{\boldsymbol{H}}(\boldsymbol{R},\boldsymbol{\lambda}_i,\boldsymbol{\rho}_i)$ is also invertible since it is a lower left-triangular matrix with positive elements on its diagonal.

IV. Indirect Adaptive Controller

In this section, a distributed indirect adaptive controller is designed for the group of agents manipulating the passive object with the aim of making the measurement point follow a given trajectory. This controller is designed to handle model parameter uncertainties and a potential loss of efficiency in the actuators of the agents. In addition, an anti-windup-like mechanism is embedded in the adaptive laws to deal with the saturation of the actuators. In the proposed solution, every agent employs a dynamic parameter estimator, consisting of an adaptive observer, to tune online the parameters of the model. The controller is distributed, since the i^{th} agent controls the portion of the dynamics that are only related to the i^{th} actuator. However, the controller is not fully decentralized, since it is required that a leader agent collects all the velocity estimates $\boldsymbol{\xi}_i \in \mathbb{R}^6$ and broadcasts the reconstructed total velocities estimate $\boldsymbol{\xi} \in \mathbb{R}^6$.

A. Adaptive Observer

The adaptive observer of the i^{th} agent has the form

$$\boldsymbol{M}(\boldsymbol{x},\hat{\boldsymbol{\theta}}_i)\dot{\boldsymbol{\xi}}_i = \hat{\boldsymbol{\tau}}_{p_i} - \boldsymbol{C}(\boldsymbol{x},\dot{\boldsymbol{x}},\hat{\boldsymbol{\theta}}_i)\boldsymbol{\xi}_i - \boldsymbol{K}_{\mathrm{obs}}(\boldsymbol{\xi}_i - \alpha_i\dot{\boldsymbol{x}}) \tag{6}$$

$$\boldsymbol{\xi}_i(0) = \boldsymbol{\xi}_{i0} \in \mathbb{R}^6$$

with

$$\begin{aligned}\hat{\boldsymbol{\tau}}_{p_i} &= \boldsymbol{H}(\boldsymbol{R},\hat{\boldsymbol{r}}_i)\hat{\boldsymbol{\Lambda}}_i\boldsymbol{u}_i = \bar{\boldsymbol{H}}(\boldsymbol{R},\hat{\boldsymbol{\lambda}}_i,\hat{\boldsymbol{\rho}}_i)\boldsymbol{u}_i \qquad (7a) \\ &= \boldsymbol{Y}_\lambda(\boldsymbol{u}_i)\hat{\boldsymbol{\lambda}}_i + \boldsymbol{Y}_\rho(\boldsymbol{R},\boldsymbol{u}_i)\hat{\boldsymbol{\rho}}_i \qquad (7b)\end{aligned}$$

where $\boldsymbol{K}_{\mathrm{obs}} \in \mathbb{R}^{6\times 6}$ is a symmetric positive definite gain matrix, $\alpha_i \in \mathbb{R}, i = 1,\dots,N$ are scalars such that $\sum_{i=1}^N \alpha_i = 1$, $\hat{\boldsymbol{\theta}}_i = \boldsymbol{\theta} + \tilde{\boldsymbol{\theta}}_i$ is the estimated inertial parameter vector with estimation error $\tilde{\boldsymbol{\theta}}_i$, $\hat{\boldsymbol{\tau}}_{p_i}$ is the estimate of the wrench applied by the agent i^{th} at the measurement point, obtained using the estimates $\hat{\boldsymbol{\lambda}}_i = \boldsymbol{\lambda}_i + \tilde{\boldsymbol{\lambda}}_i$ and $\hat{\boldsymbol{\rho}}_i = \boldsymbol{\rho}_i + \tilde{\boldsymbol{\rho}}_i$ with estimation errors $\tilde{\boldsymbol{\lambda}}_i$ and $\tilde{\boldsymbol{\rho}}_i$. In (6), the dependence of $\boldsymbol{M}(\cdot)$ and $\boldsymbol{C}(\cdot)$ on the estimated inertial parameters $\hat{\boldsymbol{\theta}}_i$ is highlighted. In addition, if $\hat{\boldsymbol{\theta}}_i$ is physically consistent then $\boldsymbol{M}(\boldsymbol{x},\hat{\boldsymbol{\theta}}_i)$ is positive definite (hence invertible).

The update laws for $\hat{\boldsymbol{\theta}}_i$, $\hat{\boldsymbol{\lambda}}_i$, $\hat{\boldsymbol{\rho}}_i$, $i = 1,\dots,N$, are selected as follows

$$\dot{\hat{\boldsymbol{\theta}}}_i = \underset{\hat{\boldsymbol{\theta}}_i \in \Theta}{\mathrm{Proj}}\{\gamma_i g^{-1}(\hat{\boldsymbol{\theta}}_i)\bar{\boldsymbol{Y}}_\theta^T(\boldsymbol{x},\dot{\boldsymbol{x}},\boldsymbol{\xi}_i,\dot{\boldsymbol{\xi}}_i)\tilde{\boldsymbol{\xi}}\} \tag{8}$$

$$\dot{\hat{\boldsymbol{\lambda}}}_i = \underset{\hat{\boldsymbol{\lambda}}_i \in \Lambda}{\mathrm{Proj}}\{-\boldsymbol{T}_i\boldsymbol{Y}_\lambda^T(\boldsymbol{u}_i)\tilde{\boldsymbol{\xi}}\} \tag{9}$$

$$\dot{\hat{\boldsymbol{\rho}}}_i = \underset{\hat{\boldsymbol{\rho}}_i \in \mathcal{R}}{\mathrm{Proj}}\{-\boldsymbol{\Upsilon}_i\boldsymbol{Y}_\rho^T(\boldsymbol{R},\boldsymbol{u}_i)\tilde{\boldsymbol{\xi}}\} \tag{10}$$

where $\hat{\boldsymbol{\theta}}_i(0) \in \mathrm{int}\{\Theta\}$, $\hat{\boldsymbol{\lambda}}_i(0) \in \mathrm{int}\{\Lambda\}$, $\hat{\boldsymbol{\rho}}_i(0) \in \mathrm{int}\{\mathcal{R}\}$, and

$$\bar{\boldsymbol{Y}}_\theta(\boldsymbol{x},\dot{\boldsymbol{x}},\boldsymbol{\xi}_i,\dot{\boldsymbol{\xi}}_i)\boldsymbol{\theta} := \boldsymbol{M}(\boldsymbol{x},\boldsymbol{\theta})\dot{\boldsymbol{\xi}}_i + \boldsymbol{C}(\boldsymbol{x},\dot{\boldsymbol{x}},\boldsymbol{\theta})\boldsymbol{\xi}_i \tag{11}$$

The variables $\tilde{\boldsymbol{\xi}}_i := \boldsymbol{\xi}_i - \alpha_i\dot{\boldsymbol{x}}$ and $\tilde{\boldsymbol{\xi}} := \sum_{i=1}^N \tilde{\boldsymbol{\xi}}_i = \sum_{i=1}^N(\boldsymbol{\xi}_i - \alpha_i\dot{\boldsymbol{x}}) = \boldsymbol{\xi} - \dot{\boldsymbol{x}}$ denote the partial and the total velocity estimation errors, respectively, $\gamma_i \in \mathbb{R}$ is a positive scalar, and $\boldsymbol{T}_i \in \mathbb{R}^{6\times 6}, \boldsymbol{\Upsilon}_i \in \mathbb{R}^{9\times 9}$ are positive definite symmetric gain matrices. The operator $\mathrm{Proj}\{\cdot\}$ is the smooth projection defined in [11] whereas $g(\cdot) \in \mathbb{R}^{10\times 10}$ is the pullback of the affine-invariant Riemannian metric on the manifold of the positive definite symmetric matrices to $\mathbb{R}^{10}$ defined in [12]. It should be noted that, since $\hat{\boldsymbol{\theta}}_i$ is projected into Θ, and the pullback $g(\hat{\boldsymbol{\theta}}_i)$ ensures that $\hat{\boldsymbol{\theta}}_i(t) \in \mathcal{M}$, then $\hat{\boldsymbol{\theta}}_i(t) \in \mathcal{M}_c$ for all $t \ge 0$. Consequently, the matrix $g(\hat{\boldsymbol{\theta}}_i(t))$ is symmetric and positive definite for all $t \ge 0$. Asymptotic convergence to zero of the errors $\tilde{\boldsymbol{\xi}}_i(t)$ is proven in Theorem 1.

B. Adaptive Controller

In this subsection, a distributed controller for the i^{th} agent is designed based on its observer dynamics. Position, orientation and velocity errors are defined with respect to a smooth reference trajectory of the rigid body at measurement point as follows

$$\begin{aligned}\tilde{\boldsymbol{p}} &= \boldsymbol{p} - \boldsymbol{p}_{\mathrm{ref}}, \quad \tilde{\boldsymbol{v}} = \boldsymbol{v} - \boldsymbol{v}_{\mathrm{ref}} \\ \tilde{\boldsymbol{R}} &= \boldsymbol{R}\boldsymbol{R}_{\mathrm{ref}}^T, \quad \tilde{\boldsymbol{\omega}} = \boldsymbol{\omega} - \tilde{\boldsymbol{R}}\boldsymbol{\omega}_{\mathrm{ref}}\end{aligned} \tag{12}$$

The kinematic relation between $\tilde{\boldsymbol{p}}$ and $\tilde{\boldsymbol{v}}$ is $\dot{\tilde{\boldsymbol{p}}} = \tilde{\boldsymbol{v}}$. The Modified Rodriguez Parameters (MRP) [13] are used to parameterize the orientation error $\tilde{\boldsymbol{R}} \in SO(3)$. Note that $\tilde{\boldsymbol{R}} = \mathbb{I}_{3\times3} \Leftrightarrow \tilde{\boldsymbol{\sigma}} = 0$. The propagation equation of the MRP is

$$\dot{\tilde{\boldsymbol{\sigma}}} = \frac{1}{2}\boldsymbol{G}(\tilde{\boldsymbol{\sigma}})\tilde{\boldsymbol{\omega}} \tag{13}$$

where $\boldsymbol{G}(\tilde{\boldsymbol{\sigma}}) := \frac{1-\tilde{\boldsymbol{\sigma}}^T\tilde{\boldsymbol{\sigma}}}{2}\mathbb{I}_{3\times3} - [\tilde{\boldsymbol{\sigma}}]_\times + [\tilde{\boldsymbol{\sigma}}]_\times^2$. Define the augmented velocity errors

$$\boldsymbol{v}_{\mathrm{err}} := \boldsymbol{v} - \boldsymbol{v}_{\mathrm{cmd}} = \boldsymbol{v} - \boldsymbol{v}_{\mathrm{ref}} + \boldsymbol{K}_{\mathrm{p}}\tilde{\boldsymbol{p}} = \tilde{\boldsymbol{v}} + \boldsymbol{K}_{\mathrm{p}}\tilde{\boldsymbol{p}} \tag{14}$$

$$\boldsymbol{\omega}_{\mathrm{err}} := \boldsymbol{\omega} - \boldsymbol{\omega}_{\mathrm{cmd}} = \boldsymbol{\omega} - \tilde{\boldsymbol{R}}\boldsymbol{\omega}_{\mathrm{ref}} + \boldsymbol{K}_\sigma\tilde{\boldsymbol{\sigma}} = \tilde{\boldsymbol{\omega}} + \boldsymbol{K}_\sigma\tilde{\boldsymbol{\sigma}} \tag{15}$$

where $\boldsymbol{v}_{\mathrm{cmd}} := \boldsymbol{v}_{\mathrm{ref}} - \boldsymbol{K}_{\mathrm{p}}\tilde{\boldsymbol{p}}$ and $\boldsymbol{\omega}_{\mathrm{cmd}} := \tilde{\boldsymbol{R}}\boldsymbol{\omega}_{\mathrm{ref}} - \boldsymbol{K}_\sigma\tilde{\boldsymbol{\sigma}}$ are the commanded linear and angular velocities, respectively, and $\boldsymbol{K}_{\mathrm{p}} \in \mathbb{R}^{3\times3}, \boldsymbol{K}_\sigma \in \mathbb{R}^{3\times3}$ are symmetric positive definite matrices. To simplify the upcoming discussion, it is convenient to define the signals $\tilde{\boldsymbol{x}} := \left[\tilde{\boldsymbol{p}}^T, \tilde{\boldsymbol{\sigma}}^T\right]^T \in \mathbb{R}^6$, $\dot{\boldsymbol{x}}_{\mathrm{err}} := \left[\boldsymbol{v}_{\mathrm{err}}^T, \boldsymbol{\omega}_{\mathrm{err}}^T\right]^T \in \mathbb{R}^6$ and $\dot{\boldsymbol{x}}_{\mathrm{cmd}} := \left[\boldsymbol{v}_{\mathrm{cmd}}^T, \boldsymbol{\omega}_{\mathrm{cmd}}^T\right]^T \in \mathbb{R}^6$. Combining equations (14), (15) and (13) the dynamics of the pose error $\tilde{\boldsymbol{x}}$ is given by

$$\dot{\tilde{\boldsymbol{p}}} = -\boldsymbol{K}_{\mathrm{p}}\tilde{\boldsymbol{p}} + \boldsymbol{v}_{\mathrm{err}}, \quad \dot{\tilde{\boldsymbol{\sigma}}} = \frac{1}{2}\boldsymbol{G}(\tilde{\boldsymbol{\sigma}})\left[-\boldsymbol{K}_\sigma\tilde{\boldsymbol{\sigma}} + \boldsymbol{\omega}_{\mathrm{err}}\right] \tag{16}$$

Proposition 1. *Assume that $\dot{\boldsymbol{x}}_{\mathrm{err}} \in \mathcal{L}_{\infty,e}$. Then, the dynamics of the position and orientation error* (16) *are ISS with respect to the inputs $\dot{\boldsymbol{v}}_{\mathrm{err}}$ and $\dot{\boldsymbol{\omega}}_{\mathrm{err}}$, respectively. In particular, the bounds*

$$||\tilde{\boldsymbol{p}}(\cdot)||_\infty \leq \max\left\{|\tilde{\boldsymbol{p}}(0)|, \frac{1}{\lambda_{\min}(\boldsymbol{K}_{\mathrm{p}})}||\boldsymbol{v}_{\mathrm{err}}(\cdot)||_\infty\right\} \tag{17a}$$

$$||\tilde{\boldsymbol{\sigma}}(\cdot)||_\infty \leq \max\left\{|\tilde{\boldsymbol{\sigma}}(0)|, \frac{1}{\lambda_{\min}(\boldsymbol{K}_\sigma)}||\boldsymbol{\omega}_{\mathrm{err}}(\cdot)||_\infty\right\} \tag{17b}$$

hold, where $\tilde{\boldsymbol{p}}(0) \in \mathbb{R}^3$, $\tilde{\boldsymbol{\sigma}}(0) \in \mathbb{R}^3$ are the initial conditions of the respective signals and $\lambda_{\min}(\cdot)$ denotes the minimum eigenvalue of the argument matrix.

Proof. The result follows immediately from [11, Lemma 3.3] applied to the Lyapunov functions $V_1(\tilde{\boldsymbol{p}}) = \frac{1}{2}\tilde{\boldsymbol{p}}^T\tilde{\boldsymbol{p}}$ and $V_2(\tilde{\boldsymbol{\sigma}}) = 2\ln(1 + \tilde{\boldsymbol{\sigma}}^T\tilde{\boldsymbol{\sigma}})$. □

As a result, it is sufficient to regulate $\dot{\boldsymbol{x}}_{\mathrm{err}}(t)$, to zero to regulate the pose error to zero. However, the dynamics of $\dot{\boldsymbol{x}}_{\mathrm{err}}$ depend on the unknown parameter $\boldsymbol{\theta}$. This can be easily noticed by substituting (1) in the expression of the time derivative of (14) and (15). To avoid the occurrence of $\boldsymbol{\theta}$, the commanded error for the i^{th} agent is defined as

$$\boldsymbol{z}_i := \boldsymbol{\xi}_i - \alpha_i\dot{\boldsymbol{x}}_{\mathrm{cmd}}, \quad i = 1, \ldots, N. \tag{18}$$

and the cumulative error as $\boldsymbol{z} := \sum_{i=1}^N \boldsymbol{z}_i$. Since

$$\boldsymbol{z} = \sum_{i=1}^N(\boldsymbol{\xi}_i - \alpha_i\dot{\boldsymbol{x}}_{\mathrm{cmd}}) = \boldsymbol{\xi} - \dot{\boldsymbol{x}}_{\mathrm{cmd}} = \tilde{\boldsymbol{\xi}} + \dot{\boldsymbol{x}}_{\mathrm{err}} \tag{19}$$

if $\tilde{\boldsymbol{\xi}}(t) \to 0$ and $\boldsymbol{z}(t) \to 0$, then also $\dot{\boldsymbol{x}}_{\mathrm{err}}(t) \to 0$ by virtue of (19). The occurrence of the former condition is provided in the proof of Theorem 1. Next, the control $\boldsymbol{u}_i^{\mathrm{cmd}}$ is designed to regulate $\boldsymbol{z}_i(t)$ to zero in absence of saturation. Substituting (6) in the time derivative of (18) yields

$$\begin{aligned}\boldsymbol{M}(\boldsymbol{x}, \hat{\boldsymbol{\theta}}_i)\dot{\boldsymbol{z}}_i = &-\boldsymbol{C}(\boldsymbol{x}, \dot{\boldsymbol{x}}, \hat{\boldsymbol{\theta}}_i)\boldsymbol{\xi}_i - \boldsymbol{K}_{\mathrm{obs}}(\boldsymbol{\xi}_i - \alpha_i\dot{\boldsymbol{x}})\\ &+ \bar{\boldsymbol{H}}(\boldsymbol{R}, \hat{\boldsymbol{\lambda}}_i, \hat{\boldsymbol{\rho}}_i)\boldsymbol{u}_i - \boldsymbol{M}(\boldsymbol{x}, \hat{\boldsymbol{\theta}}_i)\alpha_i\ddot{\boldsymbol{x}}_{\mathrm{cmd}}\end{aligned}$$

where $\boldsymbol{u}_i = \boldsymbol{u}_i^{\mathrm{cmd}} - \mathrm{dz}_i(\boldsymbol{u}_i^{\mathrm{cmd}})$, being $\mathrm{dz}_i(\cdot)$ the deadzone associated with $\mathrm{sat}_i(\cdot)$. In the following, the contribution of the deadzone to the control input is considered to be a disturbance since it can not be eliminated. The control input

$$\begin{aligned}\boldsymbol{u}_i^{\mathrm{cmd}} = \bar{\boldsymbol{H}}^{-1}(\boldsymbol{R}, \hat{\boldsymbol{\lambda}}_i, \hat{\boldsymbol{\rho}}_i)\Big[&\boldsymbol{C}(\boldsymbol{x}, \dot{\boldsymbol{x}}, \hat{\boldsymbol{\theta}}_i)\boldsymbol{\xi}_i + \boldsymbol{K}_{\mathrm{obs}}(\boldsymbol{\xi}_i - \alpha_i\dot{\boldsymbol{x}})\\ &+ \boldsymbol{M}(\boldsymbol{x}, \hat{\boldsymbol{\theta}}_i)\alpha_i\ddot{\boldsymbol{x}}_{\mathrm{cmd}} - \boldsymbol{M}(\boldsymbol{x}, \hat{\boldsymbol{\theta}}_i)\boldsymbol{N}_i\boldsymbol{z}_i\Big]\end{aligned} \tag{20}$$

where $\boldsymbol{N}_i \in \mathbb{R}^{6\times6}$ is a symmetric positive definite gain matrix, yields the closed loop dynamics

$$\dot{\boldsymbol{z}}_i = -\boldsymbol{N}_i\boldsymbol{z}_i - \boldsymbol{M}^{-1}(\boldsymbol{x}, \hat{\boldsymbol{\theta}}_i)\bar{\boldsymbol{H}}(\boldsymbol{R}, \hat{\boldsymbol{\lambda}}_i, \hat{\boldsymbol{\rho}}_i)\mathrm{dz}_i(\boldsymbol{u}_i^{\mathrm{cmd}}) \tag{21}$$

which are globally exponentially stable in absence of saturation (i.e., when $\mathrm{dz}_i(\boldsymbol{u}_i^{\mathrm{cmd}}) = 0$ for all $i = 1, \ldots, N$). The following theorem establishes the properties of the closed-loop system when no saturation occurs.

Theorem 1. *Assume that the reference trajectories satisfy $\boldsymbol{x}_{\mathrm{ref}}(\cdot)$, $\dot{\boldsymbol{x}}_{\mathrm{ref}}(\cdot)$, $\ddot{\boldsymbol{x}}_{\mathrm{ref}}(\cdot) \in \mathcal{L}_\infty$. Then, for all initial conditions $\boldsymbol{x}(0) \in SE(3)$, $\dot{\boldsymbol{x}}(0) \in \mathbb{R}^6$, $\boldsymbol{\xi}_i(0) \in \mathbb{R}^6$, $\hat{\boldsymbol{\lambda}}_i(0) \in \mathrm{int}\{\Lambda\}$, $\hat{\boldsymbol{\rho}}_i(0) \in \mathrm{int}\{\mathcal{R}\}$, and $\hat{\boldsymbol{\theta}}_i(0) \in \mathrm{int}\{\mathcal{M}_c\}$ with $i = 1, \ldots, N$ the forward trajectories of the closed-loop system given by the cascade of the observer* (6)*, the controller* (20) *and the plant* (1) *under the update laws* (8)*,* (9) *and* (10) *are bounded and satisfy*

$$||\tilde{\boldsymbol{\xi}}(\cdot)||_a = 0, \quad ||\tilde{\boldsymbol{x}}(\cdot)||_a = 0 \tag{22}$$

Proof. In order to simplify the notation, the dependency of $\boldsymbol{M}(\cdot)$ and $\boldsymbol{C}(\cdot)$ on signals $\boldsymbol{x}(t)$, $\dot{\boldsymbol{x}}(t)$ is represented by a dependency on t. Consider the Lyapunov function candidate

$$V(t, \tilde{\boldsymbol{\xi}}, \tilde{\boldsymbol{\lambda}}, \tilde{\boldsymbol{\rho}}, \tilde{\boldsymbol{\theta}}) = V_e(t, \tilde{\boldsymbol{\xi}}, \tilde{\boldsymbol{\lambda}}, \tilde{\boldsymbol{\rho}}) + V_p(\tilde{\boldsymbol{\theta}}) \tag{23}$$

where $\tilde{\boldsymbol{\lambda}} = [\tilde{\boldsymbol{\lambda}}_1^T, \ldots, \tilde{\boldsymbol{\lambda}}_N^T]^T \in \mathbb{R}^{6N}$, $\tilde{\boldsymbol{\rho}} = [\tilde{\boldsymbol{\rho}}_1^T, \ldots, \tilde{\boldsymbol{\rho}}_N^T]^T \in \mathbb{R}^{9N}$, $\tilde{\boldsymbol{\theta}} = [\tilde{\boldsymbol{\theta}}_1^T, \ldots, \tilde{\boldsymbol{\theta}}_N^T]^T \in \mathbb{R}^{10N}$ and

$$V_e = \frac{1}{2}\tilde{\boldsymbol{\xi}}^T\boldsymbol{M}(t, \boldsymbol{\theta})\tilde{\boldsymbol{\xi}} + \frac{1}{2}\sum_{i=1}^N\left(\tilde{\boldsymbol{\rho}}_i^T\boldsymbol{\Upsilon}_i^{-1}\tilde{\boldsymbol{\rho}}_i + \tilde{\boldsymbol{\lambda}}_i^T\boldsymbol{T}_i^{-1}\tilde{\boldsymbol{\lambda}}_i\right) \tag{24}$$

$$V_p = \sum_{i=1}^N \gamma_i^{-1}D_{\mathcal{M}}(\hat{\boldsymbol{\theta}}_i||\boldsymbol{\theta}) \tag{25}$$

with

$$D_{\mathcal{M}}(\hat{\boldsymbol{\theta}}_i||\boldsymbol{\theta}) = -\log\left(\frac{\det\left(f(\hat{\boldsymbol{\theta}}_i)\right)}{\det\left(f(\boldsymbol{\theta})\right)}\right) + \mathrm{tr}\left(f^{-1}(\hat{\boldsymbol{\theta}}_i)f(\boldsymbol{\theta})\right) - 4$$

$$f(\boldsymbol{\theta}) = \begin{bmatrix}0.5\ \mathrm{tr}\,(\boldsymbol{I})\ \mathbb{I}_{3\times3} - \boldsymbol{I} & \boldsymbol{h}_c\\ \boldsymbol{h}_c^T & m\end{bmatrix}$$

where V_e is related to the observer error and V_p is related to the estimation error of the inertial parameters of the manipulated object. It is well known that the inertia matrix of a rigid body satisfies the following property:

$$m_o \mathbb{I}_{6\times 6} \leq \boldsymbol{M}(\boldsymbol{x}, \boldsymbol{\theta}) \leq m_1 \mathbb{I}_{6\times 6} \quad \forall \boldsymbol{x} \in SE(3), \quad \forall \boldsymbol{\theta} \in \mathcal{M}_c$$

where $0 < m_0 \leq m_1$ and $m_0, m_1 \in \mathbb{R}$. This property, together with the fact that $\boldsymbol{\Upsilon}^{-1}$ and $\boldsymbol{T}^{-1}$ are positive definite constant matrices, imply that $V_e(\cdot)$ is positive definite, radially unbounded, and decrescent. In [9], the authors proved that the pseudo distance (25) is a suitable Lyapunov candidate function. To facilitate the next steps of the proof, notice that

$$\begin{aligned}\boldsymbol{M}(t, \boldsymbol{\theta})\dot{\tilde{\boldsymbol{\xi}}} &= \sum_{i=1}^{N} \boldsymbol{M}(t, \boldsymbol{\theta})\dot{\boldsymbol{\xi}}_i - \boldsymbol{M}(t, \boldsymbol{\theta})\ddot{\boldsymbol{x}} \\ &= \sum_{i=1}^{N} \boldsymbol{M}(t, \hat{\boldsymbol{\theta}}_i)\dot{\boldsymbol{\xi}}_i - \sum_{i=1}^{N} \boldsymbol{M}(t, \tilde{\boldsymbol{\theta}}_i)\dot{\boldsymbol{\xi}}_i - \boldsymbol{M}(t, \boldsymbol{\theta})\ddot{\boldsymbol{x}}\end{aligned}$$

Substituting the dynamics of the i^{th} observer (6) and the system dynamics (1) in the above identity leads to

$$\begin{aligned}\boldsymbol{M}(t, \boldsymbol{\theta})\dot{\tilde{\boldsymbol{\xi}}} = &\sum_{i=1}^{N} \left[\hat{\boldsymbol{\tau}}_{p_i} - \boldsymbol{C}(t, \hat{\boldsymbol{\theta}}_i)\boldsymbol{\xi}_i - \boldsymbol{K}_{\text{obs}}(\boldsymbol{\xi}_i - \alpha_i \dot{\boldsymbol{x}})\right] \\ &- \sum_{i=1}^{N} \boldsymbol{M}(t, \tilde{\boldsymbol{\theta}}_i)\dot{\boldsymbol{\xi}}_i + \boldsymbol{C}(t, \boldsymbol{\theta})\dot{\boldsymbol{x}} - \boldsymbol{\tau}_p\end{aligned}$$

Easy but tedious computations lead to the following inequality for the Lyapunov equation:

$$\dot{V}_e \leq -\tilde{\boldsymbol{\xi}}^T \boldsymbol{K}_{\text{obs}} \tilde{\boldsymbol{\xi}} - \sum_{i=1}^{N} \boldsymbol{\xi}^T \boldsymbol{Y}_\theta(\boldsymbol{x}, \dot{\boldsymbol{x}}, \boldsymbol{\xi}_i, \dot{\boldsymbol{\xi}}_i)\tilde{\boldsymbol{\theta}}_i \tag{26}$$

In [9], it is proven that the Lie derivative of V_p is

$$\dot{V}_p = \sum_{i=1}^{N} \gamma_i^{-1} \dot{\hat{\boldsymbol{\theta}}}_i^T g(\hat{\boldsymbol{\theta}}_i)\tilde{\boldsymbol{\theta}}_i \tag{27}$$

Substituting the update law of the inertial parameter estimates in (27) and using the properties of the projection operator, one obtains

$$\dot{V}_p \leq \sum_{i=1}^{N} \tilde{\boldsymbol{\xi}}^T \boldsymbol{Y}_\theta(\boldsymbol{x}, \dot{\boldsymbol{x}}, \boldsymbol{\xi}_i, \dot{\boldsymbol{\xi}}_i)\tilde{\boldsymbol{\theta}}_i \tag{28}$$

Combining (28) and (26) the Lie derivative of V is bounded as follows

$$\dot{V} \leq -\tilde{\boldsymbol{\xi}}^T \boldsymbol{K}_{obs} \tilde{\boldsymbol{\xi}} \leq 0 \tag{29}$$

Equation (29) implies that for all $\boldsymbol{\xi}(0), \hat{\boldsymbol{\lambda}}(0), \hat{\boldsymbol{\rho}}(0), \hat{\boldsymbol{\theta}}(0)$

$$V(t, \tilde{\boldsymbol{\xi}}(t), \tilde{\boldsymbol{\lambda}}(t), \tilde{\boldsymbol{\rho}}(t), \tilde{\boldsymbol{\theta}}(t)) \leq V(0, \tilde{\boldsymbol{\xi}}(0), \tilde{\boldsymbol{\lambda}}(0), \tilde{\boldsymbol{\rho}}(0), \tilde{\boldsymbol{\theta}}(0))$$

for all $t \in [0, T_{\max})$ where $T_{\max}$ is the maximal interval of existence and uniqueness of the forward trajectories of the overall closed-loop system. It is then easy to show that the previously defined bounds lead to the conclusion that all signals are bounded over the maximal interval $[0, T_{\max})$, hence $T_{\max} = +\infty$. Convergence of the velocity estimation error $\tilde{\boldsymbol{\xi}}(t)$ is proven applying LaSalle/Yoshizawa theorem to the Lyapunov function (23). This fact, together with the exponential stability of (21) and the identity (19) prove that $\dot{\boldsymbol{x}}_{\text{err}}(t)$ converges asymptotically. Convergence of the pose error $\tilde{\boldsymbol{x}}(t)$ follows by Proposition 1. □

TABLE I: Direct Adaptive Controller Performance

	Scenario 1	Scenario 2
Position Err. [mm]	0.851	1.56
Orientation Err. $\times 10^{-3}$	0.501	0.894
Fuel Force [N^2 s]	140.9	132.7
Fuel Torque [$\mathrm{N}^2\mathrm{m}^2$ s]	460.7	457.9

V. Simulations

The performance of the adaptive controller proposed in this work is evaluated in comparative simulations with the direct adaptive controller presented in [8]. A challenging scenario is considered to evaluate the effects of the actuators nonlinearities on the stability of the closed-loop system. In particular, a scenario where a group of $N = 4$ space robots are manipulating a cube-shaped passive object is considered.

A. Simulation Setup

Simulations are performed in the Matlab-Simulink® environment using the Mechanics toolbox. A one-meter-long cube is considered as passive manipulated object. The measurement point is placed at the center of one of the cube faces, where the z-axis of the frame $\mathcal{P}$ is aligned with the normal outward vector, and the other two axes are aligned with the cube sides. A white Gaussian noise with zero mean and standard deviation $\sigma = 10^{-3}$ is added to the measured position, attitude, and velocities signals to simulate sensor noise. The assigned reference trajectory makes the geometric center of the passive object move along an eight-shaped path. The trajectory is periodic in the spatial domain with respect to the geometric center of the manipulated object, and requires continuous application of a control wrench. During the reference motion, the object is rotated three times along the path. The gains of the controller proposed in this work and of the one presented in [8] have been tuned to obtain similar closed-loop performance in terms of regulated error and energy consumption in absence of loss of efficiency and saturation of the actuators. To ensure a fair comparison, the natural adaptive law of [9] is employed in the update of the estimated inertial parameters of the passive object for the adaptive controller of [8] as well.

B. Comparative Simulation Study

First, a scenario with nominal actuator efficiency, $\boldsymbol{\Lambda}_i = \mathbb{I}_{6\times 6}$, and no saturation is considered to establish a baseline for comparison. Table I and Table II present (for both controllers) the average of the norm of the position and orientation errors along with the integral of the norm-squared of the control wrenches applied to the object. A similar performance is obtained by the two controllers, as it can be inferred from the reported data.

The second scenario concerns the analysis of the effect of a partial failure of the actuation system of two agents

TABLE II: Indirect Adaptive Controller Performance

	Scenario 1	Scenario 2	Scenario 3
Position Err. [mm]	1.11	1.35	12.6
Orientation Err. $\times 10^{-3}$	0.503	1.3	1.69
Fuel Force [$\mathrm{N}^2\,\mathrm{s}$]	118.2	114.7	119.1
Fuel Torque [$\mathrm{N}^2\mathrm{m}^2\,\mathrm{s}$]	457.1	453.2	467.3

occurring at $t = 85$ [s] during a simulation employing the same reference trajectory as the baseline case. Specifically, the actuator efficiency of agent no. 2 is reduced by 70 % in all directions of the input space, and the control efficiency for agent no. 4 is reduced by 70 % along the x-axis and by 50 % along the y-axis, both in terms of force and torque exerted on the object. A comparable level of performance for both controllers is evident from the data reported in Table I and Table II. Finally, the effect of actuator saturations on the performance of the two controllers are studied in the third scenario. In addition to the setup considered in the second simulation, herein a maximum deliverable force of 0.5 [N] and a maximum deliverable torque of 0.5 [Nm] along each axis is imposed on each agent. In this case, after the time instant $t = 85$ [s] when the efficiency loss occurs, agents no. 1 and no. 3 are required to apply a larger control wrench than the nominal one, which results in these two agents hitting their actuator saturation limits. As a consequence, the direct controller fails to maintain closed-loop stability, as its update law reacts abnormally to the occurrence of actuator saturation, which is interpreted as a parameter variation, resulting in a behavior akin to integrator wind-up (see the bottom plot of Figure 2). Conversely, the indirect controller uses the correct information on the actuator behavior in the regressor employed in the update law, hence the dynamics of the parameter estimates do not exhibit integrator wind-up – see the top plot of Figure 2. As expected, the tracking performance worsens while the saturations are active, as can be noticed from the average position and orientation errors reported in Table II, but regulation is recovered once nominal operating conditions are restored.

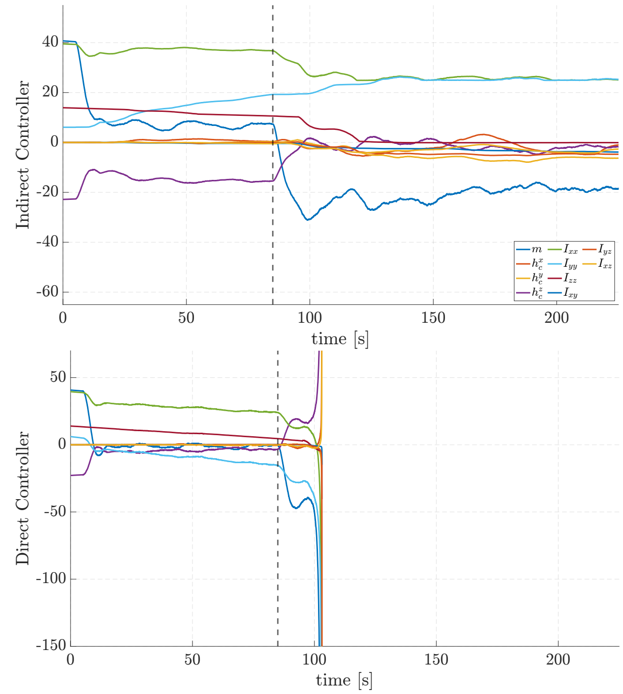

Fig. 2: Time history of the estimation error of the inertial parameters in the third simulation scenario. The vertical dashed line marks the time instant $t = 85$ [s] when the actuator efficiency of agents no. 2 and no. 4 is reduced.

VI. Conclusions

A distributed indirect adaptive controller has been proposed for trajectory tracking of a passive object manipulated cooperatively by a group of robotic agents. The controller architecture is comprised of a distributed observer that is centrally coordinated by a leading agent, which has the purpose of realizing a distributed dynamic update law for the adaptive control action performed by each agent. The advantage of the scheme with respect to distributed direct control schemes lies in enhanced robustness against saturation and loss of effectiveness of the actuators. Comparative simulation studies have shown the advantages of the proposed approach versus state-of-the-art distributed direct adaptive solutions in terms of robustness with respect to actuator uncertainty.

References

[1] F. Caccavale and M. Uchiyama, “Cooperative manipulation,” *Springer Handbook of Robotics*, pp. 989–1006, 2016.

[2] A. Petitti, A. Franchi, D. Di Paola, and A. Rizzo, “Decentralized motion control for cooperative manipulation with a team of networked mobile manipulators,” in *Proceedings of the 2016 IEEE International Conference on Robotics and Automation (ICRA)*, 2016, pp. 441–446.

[3] A. Marino, G. Muscio, and F. Pierri, “Distributed cooperative object parameter estimation and manipulation without explicit communication,” in *Proceedings of the 2017 IEEE International Conference on Robotics and Automation (ICRA)*, 2017, pp. 2110–2116.

[4] P. Budde gen. Dohmann and S. Hirche, “Distributed control for cooperative manipulation with event-triggered communication,” *IEEE Transactions on Robotics*, vol. 36, no. 4, pp. 1038–1052, 2020.

[5] M. Zribi and S. Ahmad, “Adaptive control for multiple cooperative robot arms,” in *Proceedings of the 31st IEEE Conference on Decision and Control*, 1992, pp. 1392–1398.

[6] Z. Li, S. S. Ge, and Z. Wang, “Robust adaptive control of coordinated multiple mobile manipulators,” *Mechatronics*, vol. 18, no. 5-6, pp. 239–250, 2008.

[7] C. K. Verginis, M. Mastellaro, and D. V. Dimarogonas, “Robust quaternion-based cooperative manipulation without force/torque information,” *IFAC-PapersOnLine*, vol. 50, no. 1, pp. 1754–1759, 2017.

[8] P. Culbertson, J.-J. Slotine, and M. Schwager, “Decentralized adaptive control for collaborative manipulation of rigid bodies,” *IEEE Transactions on Robotics*, vol. 37, no. 6, pp. 1906–1920, 2021.

[9] T. Lee, J. Kwon, and F. C. Park, “A natural adaptive control law for robot manipulators,” in *Proceedings of the 2018 IEEE/RSJ International Conference on Intelligent Robots and Systems (IROS)*, 2018, pp. 1–9.

[10] P. M. Wensing, S. Kim, and J.-J. E. Slotine, “Linear matrix inequalities for physically consistent inertial parameter identification: A statistical perspective on the mass distribution,” *IEEE Robotics and Automation Letters*, vol. 3, no. 1, pp. 60–67, 2017.

[11] A. R. Teel, “A nonlinear small gain theorem for the analysis of control systems with saturation,” *IEEE Transactions on Automatic Control*, vol. 41, no. 9, pp. 1256–1270, 1996.

[12] J.-B. Pomet and L. Praly, “Adaptive nonlinear regulation: estimation from the Lyapunov equation,” *IEEE Transactions on Automatic Control*, vol. 37, no. 6, pp. 729–740, 1992.

[13] P. Tsiotras, “Stabilization and optimality results for the attitude control problem,” *Journal of Guidance, Control, and Dynamics*, vol. 19, no. 4, pp. 772–779, 1996.